

## Introduction

SARS-CoV-2 coronavirus relies on various enzymes to replicate effectively. Two cysteine proteases, namely 3CLpro/Mpro and P1pro are responsible for cleaving the polyproteins, to create the necessary viral proteins for building new viral particles. These proteins have been identified as potential targets for discovering therapeutic agents, and they have garnered significant attention in the drug discovery field, with much emphasis placed on understanding their structural biology and developing inhibitors.

Flare™ FEP, Cresset's new and reliable tool for binding affinity predictions, was used to study a dataset of compounds with known experimental activity reported against Mpro of SARS-CoV-2.<sup>1-4</sup> We aim to elucidate the binding affinity of these compounds to Mpro and to identify the key interactions that contribute to potency.

## Methods

Relative free energies of binding ( $\Delta\Delta G$ ) were obtained with Flare FEP by mutating the ligand in its intermediate states for both the protein-ligand complex in water and the unbound ligand.

- Small molecule forcefield: OpenFF 2.0.0
- Protein forcefield: AMBER FF14SB
- Charge method: AM1-BCC
- Solvent: Explicit TIP3P water
- Initial simulation length per  $\lambda$  window: 4ns

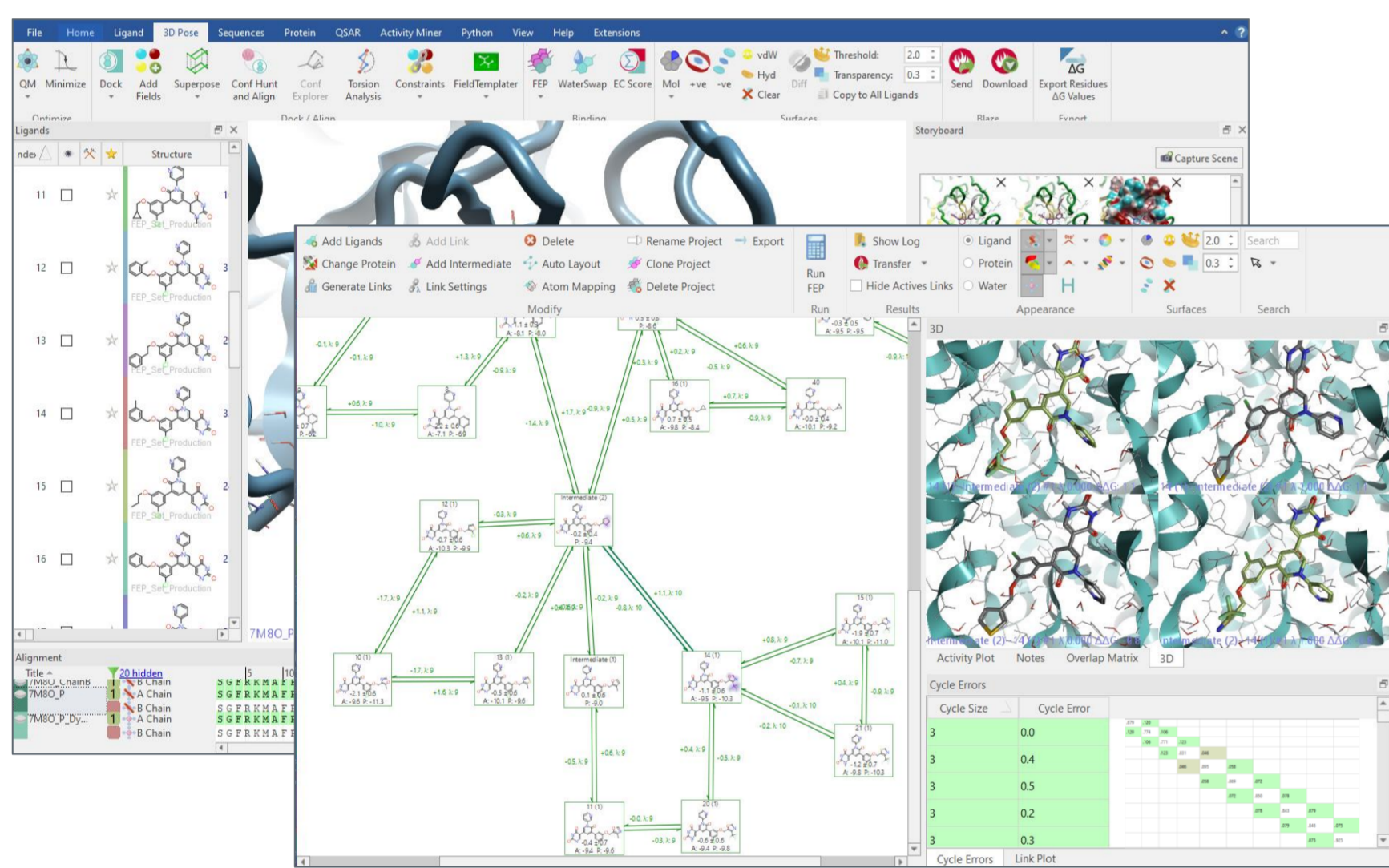


Figure 1: The user-friendly interface of Flare makes FEP calculations easy to run and troubleshoot.

## Datasets

A selection of protein crystal structures and co-crystallized ligands were evaluated. The selection was made based on the structure similarity of the ligands.

PDB Code	Resolution	Ligand	IC <sub>50</sub> of Ligand (μM)	Type of Protein	Missing loops
7M91	1.95Å	25 AYU4 401	0.025	Monomer: Chain A	Yes
7M90	2.19Å	50	0.25	Monomer: Chain A	Yes
7M8Z	1.79Å	29 AYTV 401	0.25	Monomer: Chain A	Yes
7M8P	2.23Å	23	0.02	Dimer	Yes
7M8O	2.44Å	19 AYSM 401	0.037	Dimer	No
7M8N	1.96Å	16	0.1	Dimer	Yes
7L14	1.80Å	26 AXFD 400	0.170	Dimer	Yes
7M8Y	1.75Å	15 AYTM 401	0.110	Monomer: Chain A	Yes

Table 1: Information about crystallographic data associated with this study. The red box indicates the starting point for our calculations.

PDB 7M8O with co-crystallized ligand A YSM 401 were chosen:

- No missing loops
- Stable Dynamics as monomer and as dimer

## Protein- Ligand Interactions

The co-crystallized ligand has a cloverleaf motif with a central pyridinone ring:

- Phenyl: Pocket S1
- Uracil: Pocket S1'
- Pyridinyl: Pocket S2

In this study we will explore the contribution of substituents towards the S4 pocket.

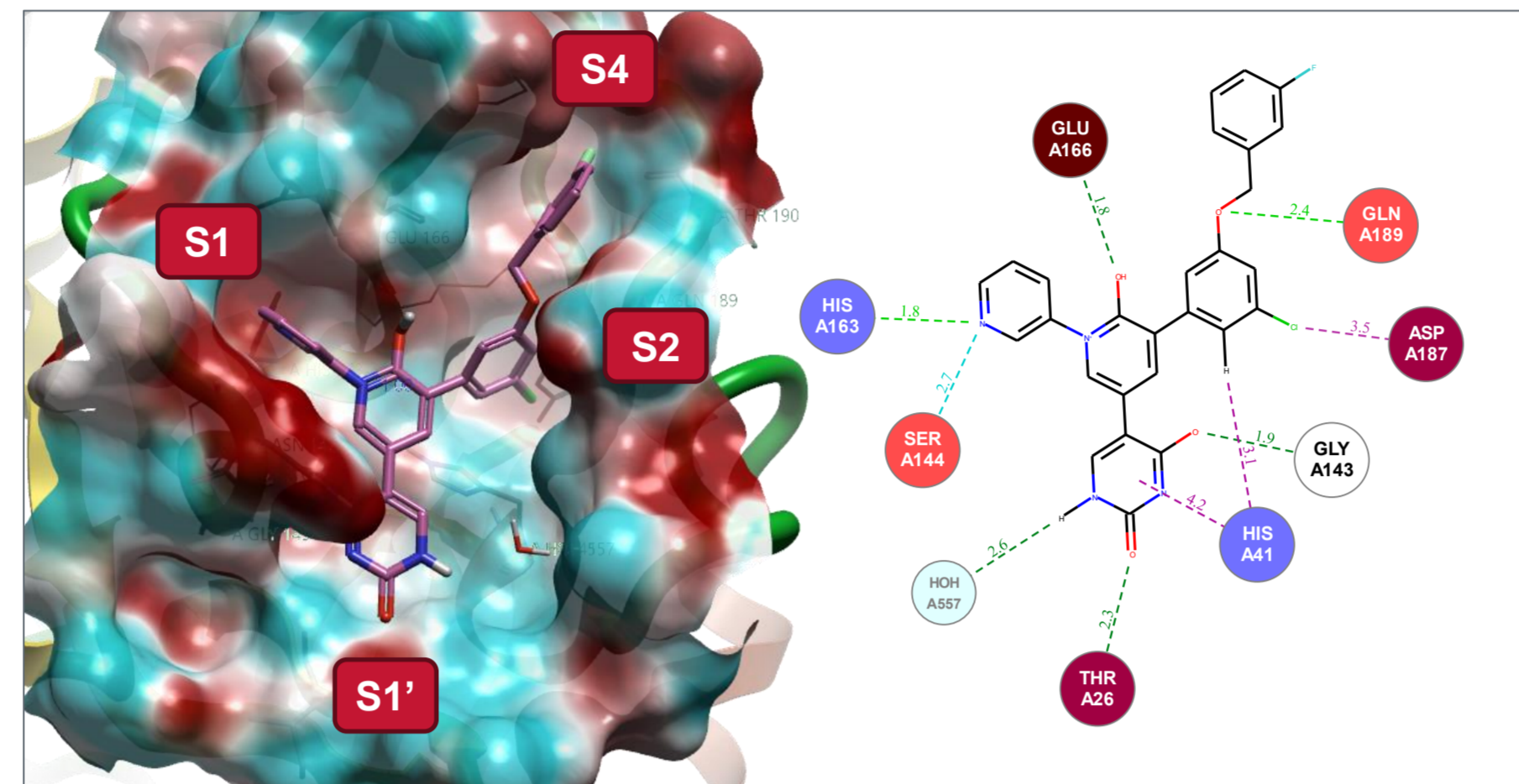


Figure 2: Left: The co-crystallized ligand explores four smaller pockets. Right: Protein- ligand interactions. Purple: Aromatic edge-to-face, Light Purple: Halogen bond, Light/ Dark Green: Strong H-bond/ H-Bond, Light Blue: Weak H-Bond

## Benchmark FEP

An evaluation of a total of 54 compounds, with IC50 values reported, was performed to select the most suitable dataset to perform FEP calculations in Flare.

A total of 36 analogues were found more suitable to generate a dataset of compounds that could be used for the FEP calculation.

- Uracil derivatives (28)
- 5-member ring (8)

The 36 compounds were aligned to A YSM 401 (PDB 7M8O co-crystallized ligand) using the 'Conformation Hunt and Alignment' method in Flare.

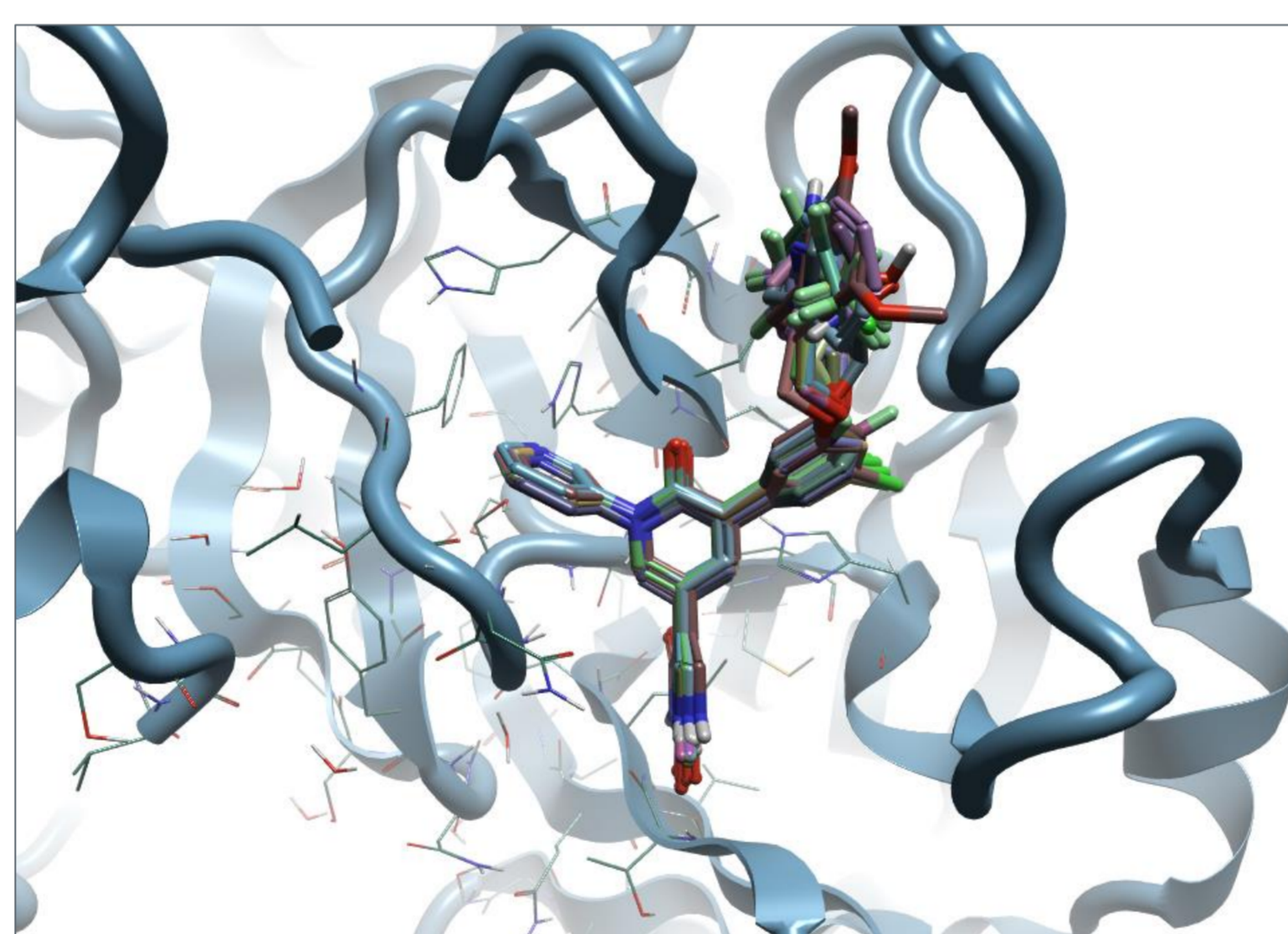


Figure 3: The analogues must be well-aligned in the binding pocket. This can be easily done with the Maximum Common Substructure (MCS) alignment method in Flare.

A well-connected perturbation network with three intermediate molecules was generated for the benchmark FEP run. The FEP graph is generated with LOMAP.<sup>5</sup>

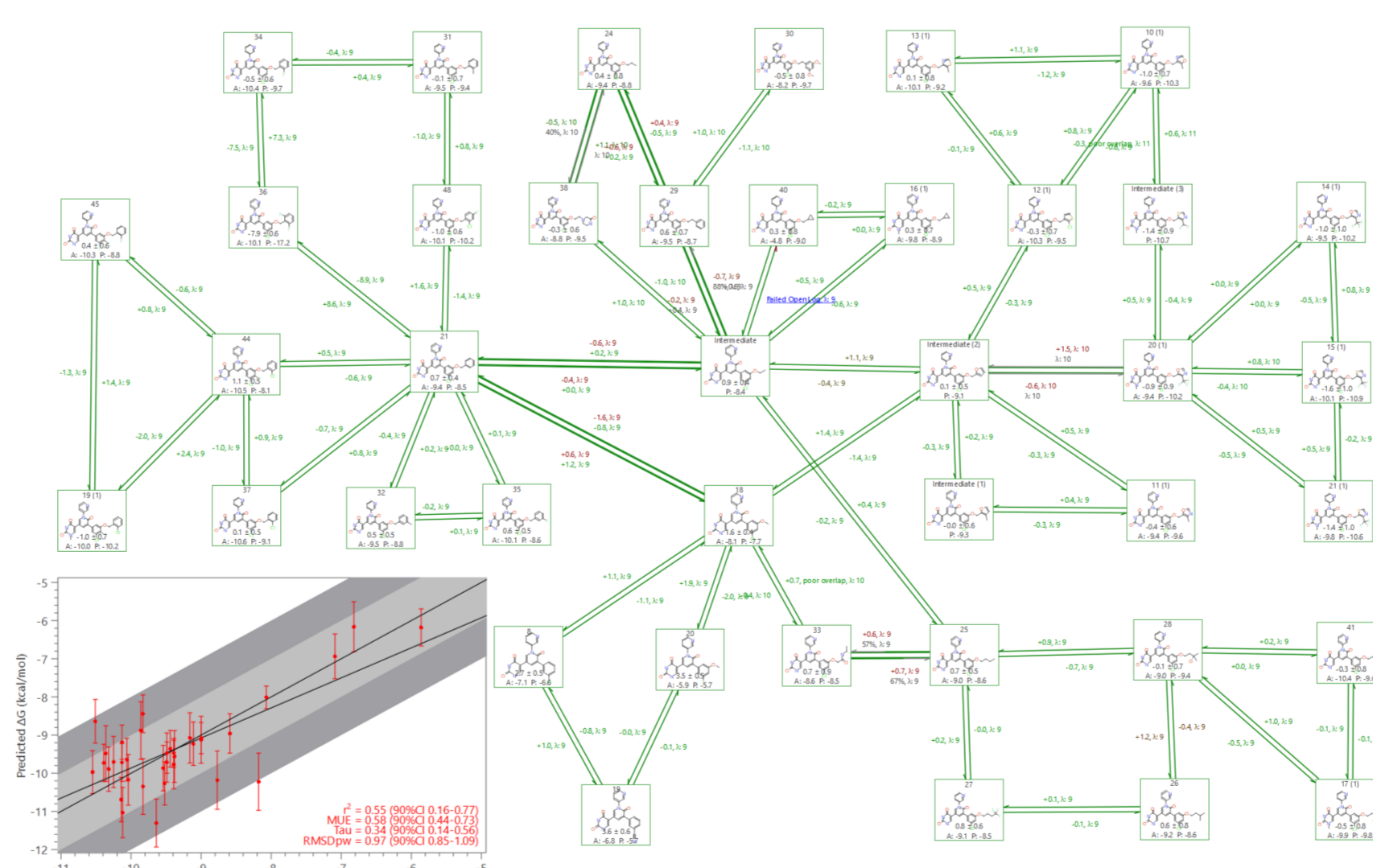


Figure 4: FEP perturbation map for the benchmark dataset. On the bottom left, the activity plot shows good correlation between experimental and predicted affinities.

Ideally the calculated  $\Delta\Delta G$  between ligands should be similar to the difference in the experimental  $\Delta G$  values, and the calculated  $\Delta G$  values should be within 1 kcal/mol from the experimentally determined  $\Delta G$ . In our case good correlation with experimental data and errors below the scientific consensus of 1 kcal/mol were found:

- $r^2 = 0.55$
- $MUE = 0.58$
- $\tau = 0.34$
- $RMSD = 0.97$

## Bioisosteric Replacement

Spark™, Cresset's bioisosteric replacement software was used to generate new designs for the production run. Spark uses 3D electrostatic and shape properties to explore R-groups on a given scaffold. Results are prioritized based on 3D similarity scores, optionally using a protein as an excluded volume.

Compound 21 was used as a starting point:

- Medium activity ( $IC_{50} = 128$  nM)
- Benzylic moiety is of interest for exploration of de-novo compounds

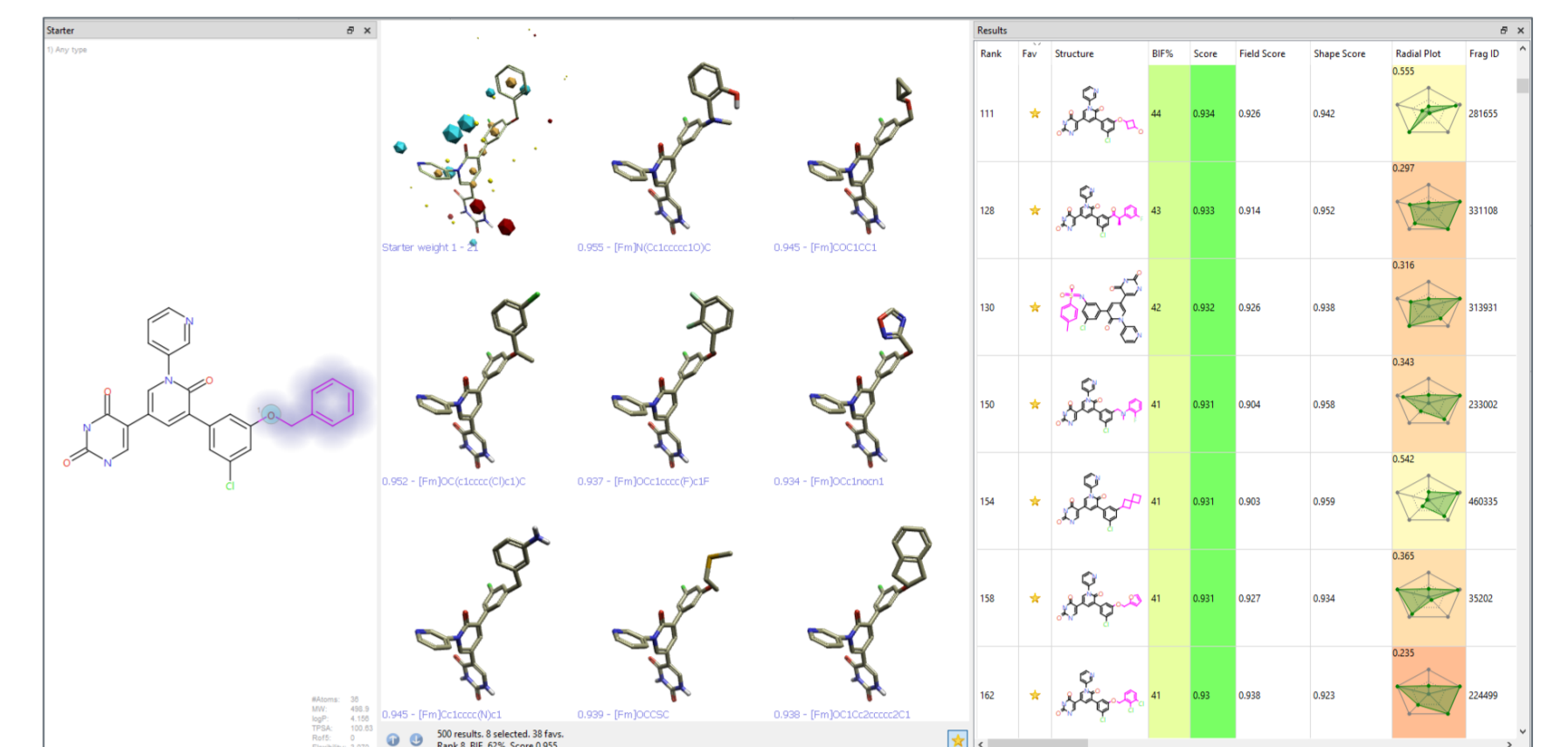


Figure 5: Results of a Spark bioisosteric R-group replacement experiment for compound 21.

From a total of 500 compounds generated, 27 were selected for the FEP prediction run based on: formal charge=0, low 2D similarity towards Compound 21, balanced calculated physicochemical properties, and meaningful chemical modifications for an FEP study.

## Production FEP

An FEP Production run with the 27 new compounds and four compounds with known activity was conducted. From the FEP production run, 13 compounds were predicted to be **more active** (10-fold more potent) than the reference Compound 21 ( $\Delta G < 9.4$  kcal/mol) and to have similar activity to the most active analogue of the entire dataset (Compound 37,  $\Delta G = 10.6$  kcal/mol).

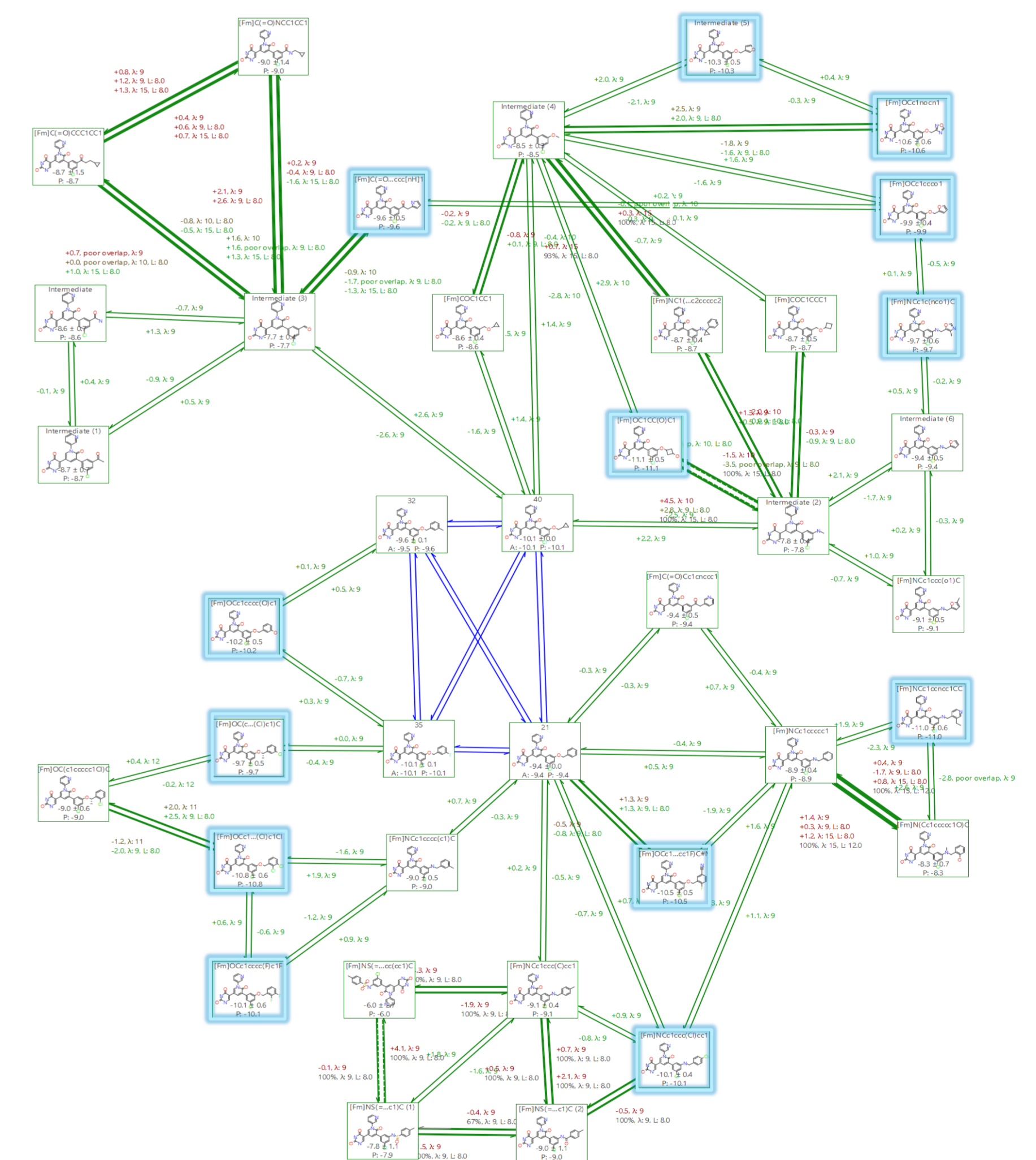


Figure 6: FEP production of 27 compounds generated from Spark, 4 compounds from the benchmark (connected with blue links) and 4 intermediate molecules.

Interesting observations:

- The amino linker is well tolerated compared to the O
- S4 pocket prefers halogen substituted phenyl groups

## Conclusions

- Flare FEP accurately predicts the binding affinity of small molecules to Mpro and can be used for binding studies of new designs
- Spark can generate new designs with high activity
- Cresset tools in synergy represent a promising approach for accelerating the discovery of new drugs

## References

1. Chun-Hui Zhang, *et al.*, ACS Cent. Sci. **2021**, 7, 467–475
2. Chun-Hui Zhang, *et al.*, ACS Med. Chem. Lett. **2021**, 12, 1325–1332
3. Maya G. Deshmukh, *et al.*, Structure **2021**, 29, 823–833, August 5, 2021
4. William L. Jorgensen, WO 2022/150584 A1
5. David L. Mobley, *et al.*, J. Comput. Aided Mol. Des., **2013**, 27, 9, 755-770